



PAUL SCHERRER INSTITUT



**SLS-TME-TA-1998-0004**  
**March 1998**

# **Eddy current calculations for the SLS corrector magnets**

**M. Dehler**

**PSI**

# Eddy current calculations for the SLS corrector magnets

Micha Dehler

In the SLS design, it is envisaged to use a combined corrector/sextupole magnet design, where additional corrector coils are placed inside the sextupole magnet producing the necessary dipole fields. The correctors are part of the feed back scheme, planned to run in the 50-100 Hz regime.

The response of the magnetic field due to the time varying current in the corrector coils is influenced mainly by two effects. The first one is the time delay and attenuation caused by eddy currents in the lamination of the magnet yoke. Additionally, there are eddy current losses on the surface of the vacuum chamber leading to a further deterioration of the behavior.

In principle, there is also an inductive coupling between the sextupole and the corrector coils to consider. There is a voltage induced in the sextupole windings and, if e.g. the sextupole coils were connected in parallel to the power supply, the impedance of the power supply would influence the time domain response as well as the spatial distribution of the corrector field.

## **Eddy current losses in the magnet core**

Since the yoke consists of material with a high permeability, the attenuation and complex phase change of the field will not lead to a qualitative change in the field distribution, only the overall amplitude will be affected. The eddy current losses inside the yoke are mainly determined by the type of the material used and the thickness of the lamination.

The buildup of the magnetic flux in the magnet core happens in two steps. First the field induced by the coils propagates into the spaces between the metal sheets, a process, which happens within picoseconds. In the second step the magnetic field enters the sheet material itself. Here the bulk of attenuation and delay due to eddy currents takes place.

As is shown in figure 2, this second step can be described as a one dimensional problem, where the field distribution in the sheet is sought, subject to the boundary

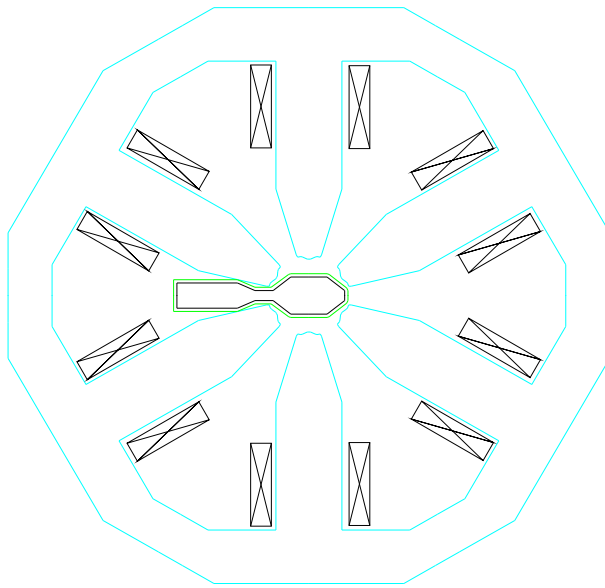


Figure 1: Sextupole magnet with vacuum chamber

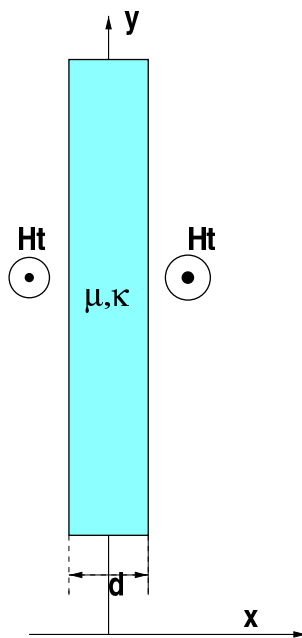


Figure 2: Magnetic sheet

conditions on the surface:

$$H(x = \pm d) = H_t$$

The field propagation inside the sheet is described by the propagation constant

$$k^2 = \omega^2 \epsilon \mu - j \omega \mu \kappa,$$

which can be approximated for low frequencies by

$$k^2 = -j \omega \mu \kappa.$$

The final distribution of the magnetic field is given by:

$$H(x) = H_t \frac{\cos(kx)}{\cos(kd/2)}$$

For the overall effect, the integral flux has to be calculated giving

$$\Psi = 2 \int_0^{d/2} B dx = \mu H_t \frac{2}{k} \tan(kd/2)$$

or, normalized by the static value for  $\omega = 0$ :

$$\Psi/\Psi_0 = \frac{2}{kd} \tan(kd/2)$$

As a material for the yoke, it is planned to use the E.B.G. steel reference 1200-100A. For the (linear) calculation, the maximum permeability of the nonlinear curve with  $\mu = 3500$  was used. Since the corrector coils are only driven in the small signal domain, remagnetization losses were neglected and only the eddy current losses taken into account. The conductivity itself was not specified on the data sheet, so it was derived from a formula by M. Werner [2], specifying the resistivity as a function of the content of silicon as

$$\rho = (9.9 + 12P_{Si}) \mu\Omega \text{ cm},$$

where  $P_{Si}$  is the content of silicon in percent. With  $P_{Si} = 1.3\%$  this gives a conductivity of approximately:

$$\kappa \approx 4 \cdot 10^6 \frac{1}{\Omega m}$$

The resulting frequency domain behavior is shown in figure 3 for different sheet thicknesses. Whereas a sheet thickness of 0.5 mm does not affect the frequency response up to 100 Hz at all, the response degrades more and more for larger thickness. A sheet thickness of 1 mm still provides a reasonable performance, whereas 2 mm thickness is unacceptable.



Figure 3: Absolute value and complex phase shift of the magnetic flux versus frequency. Sheet thickness  $d = 0.5, 1, 2$ mm. Material parameters:  $\mu = 3500$ ,  $\kappa = 4 \cdot 10^6$

## Eddy current losses in the vacuum chamber

The losses due to the eddy currents were calculated via the MAFIA program W3, which solves Maxwell's equations in the frequency domain and is specially suited to handle this kind of problem. Nonlinearities in the permeability of the yoke were neglected.

The eddy current losses in the lamination were already treated analytically in the last section and were omitted from the MAFIA model. The computations were performed in two dimensions assuming an infinitely long structure along the beam axis. For comparison, a few three dimensional calculation were done showing only minor deviations of the results, so that the use of a two dimensional model, being simpler in computational terms, is justified. The vacuum chamber consists of stainless steel with the electrical parameters  $\mu_r = 1$  and  $\kappa = 9.2 \cdot 10^6 \frac{1}{\Omega m}$  at  $20^\circ$  C temperature.

Due to the shape of the yoke and the vacuum chamber, horizontal and vertical polarizations have distinct properties, leading to differing attenuations and phase shifts of the magnetic field.

### Horizontal polarization

For the horizontal polarization, the currents driving the corrector coils are proportionally  $\cos \phi_i$  with  $\phi_i = \pi/6 + i\pi/3$ , that is, the dipole field is generated by the pair of coils at  $\phi = \pm\pi/6$  and  $\phi = \pi \pm \pi/6$  with the current in the vertical coil being zero.

Plots of the field distribution and eddy current losses are shown in figures 4 and 5. Since the symmetry plane is parallel to the dipole field, the resulting field carries only multi-pole moments of odd order  $m = 1, 3, 5 \dots$ , the behaviour of the multipole components have not been calculated.

The resulting attenuations and phase shifts are relatively small compared to the effect caused by the losses in the magnet core, as can be seen in figure 6. In a first order approximation. the typical time constant is 1.8 milliseconds including the magnet core losses.

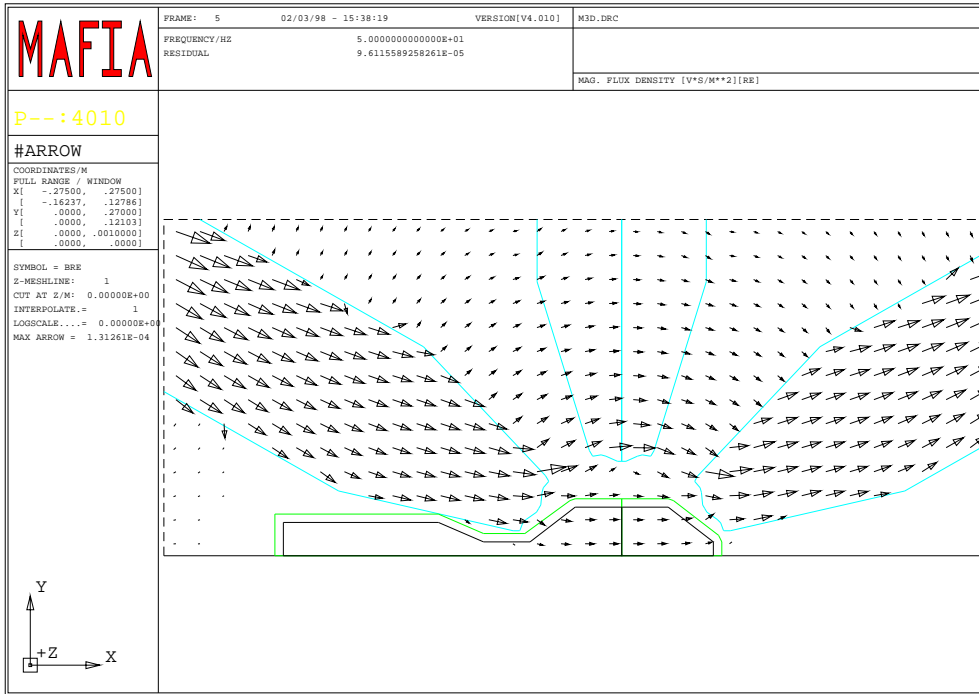


Figure 4: Horizontal polarization: Real part of the magnetic flux density at 50 Hz

## Vertical polarization

In this case, the coils are driven with a current distribution proportional  $\sin\phi_i$  with  $\phi_i = \pi/6 + i\pi/3$ , that is, all coils contribute to the magnetic field.

As can be seen in figure 7, the eddy current losses are widely distributed across the chamber wall and show a stronger effect than in the horizontal case. The corresponding attenuations and phase shifts can be seen in figure 8. The combined effects of chamber losses and magnet losses seems to be just at the limit of the necessary performance for the corrector magnet. A first order approximation gives a time constant of 6.4 milliseconds for the transition into steady state.

The photon channel distorts the symmetry of the current distribution of the vacuum chamber, giving rise to an additional quadrupole momentum in the magnetic field. As can be seen in figures 9 and 10, this effect is negligible for very low frequencies – or low losses – and increases with the frequency to be quite pronounced at 50 Hz.

There being no losses at zero frequency, the resulting quadrupole moment, shown in figure 11, starts growing linearly from zero, before increasing eddy currents start to shield the beam region from the incident field. Where the dipole field shows a time domain response with respect to a step in the current proportional  $1 - e^{-t/\tau}$ , the quadrupole behaves more like the derivative  $e^{-t/\tau}$ , performing a jump – moderated by the build up time of the field in the magnet core – followed by a slow exponen-

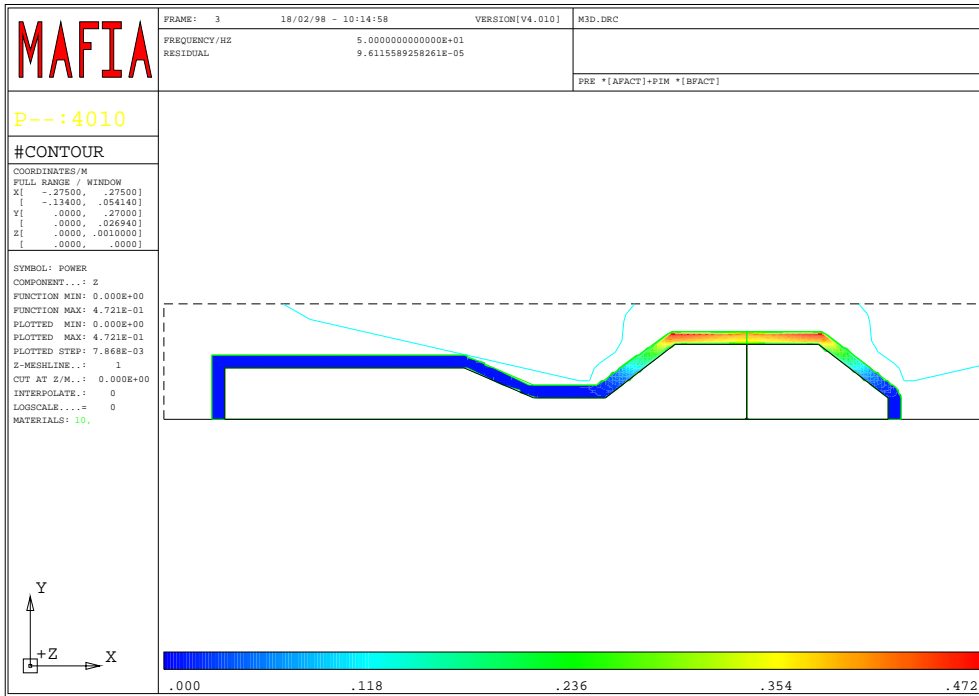


Figure 5: Horizontal polarization: Eddy current loss density on the vacuum chamber walls at 50 Hz

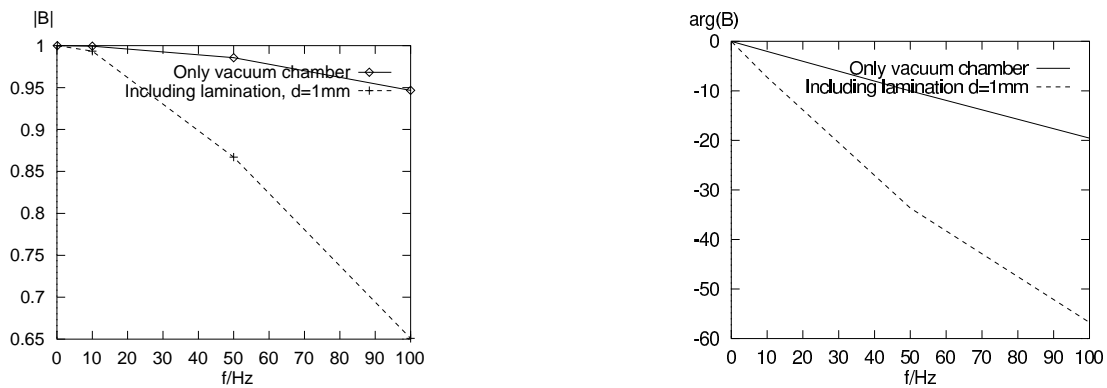


Figure 6: Horizontal polarization: Normalized amplitude and phase of the magnetic field on the beam axis versus frequency. Two cases are shown, one including only losses on the chamber wall, the other adding the losses in the magnet core.

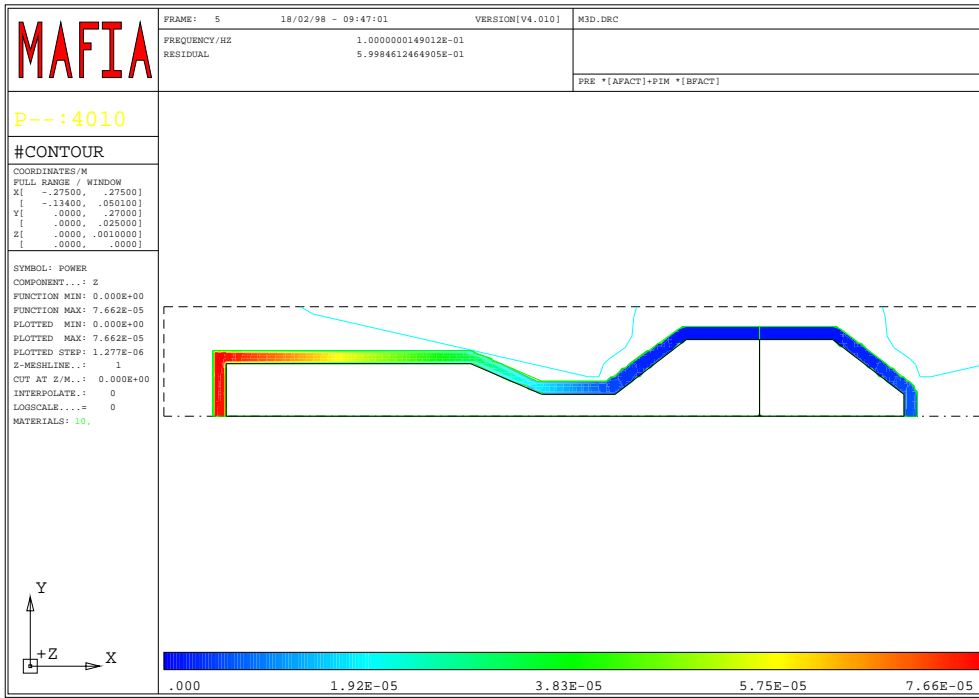


Figure 7: Vertical polarization: Eddy current losses in the vacuum chamber at 50 Hz

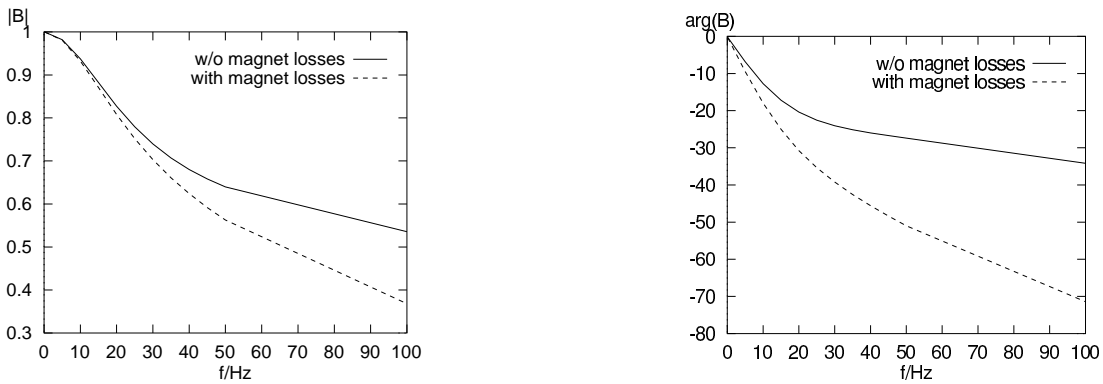


Figure 8: Vertical polarization: Normalized amplitude and phase of the magnetic field on the beam axis versus frequency. Two cases are shown, one including only eddy current losses in the vacuum chamber, the other adding the losses in the magnet core.

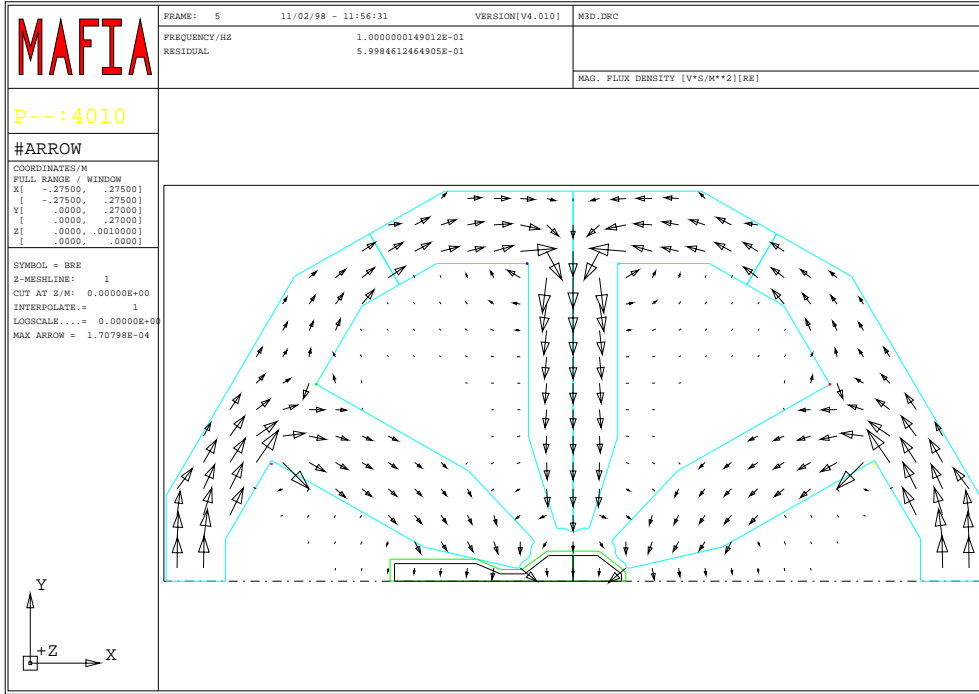


Figure 9: Vertical polarization: Distribution of the magnetic flux at 0.1 Hz

tial decrease down to zero. From the frequency domain variation of the quadrupole momentum, the peak value of the quadrupole effect is estimated to be

$$\frac{1}{B_{dipole}(t \rightarrow \infty)} \frac{d\hat{B}}{dx} \Big|_{t=0} \approx 13m^{-1},$$

where  $B_{dipole}(t \rightarrow \infty)$  is the steady state strength of the dipole field.

In principle, a possible fix for this would be to add additional steel sheets to the right side of the chamber, that way creating additional eddy currents helping to balance the magnetic field distribution, but leading to a stronger attenuation.

A second alternative would be to use a different distribution of exciting currents, such as powering only the coils on the vertical poles. This configuration leads to a more symmetric distribution of the eddy currents with a lower integral loss. Apart from a smaller quadrupole moment, also the frequency behaviour of the dipole field itself would be strongly improved. Since the distribution of the driving currents does not correspond to the ideal one, a drawback in form of an increased sextupole moment in the static field distribution is to be expected.

An examination of the influence of these spurious effects follows in the next section.

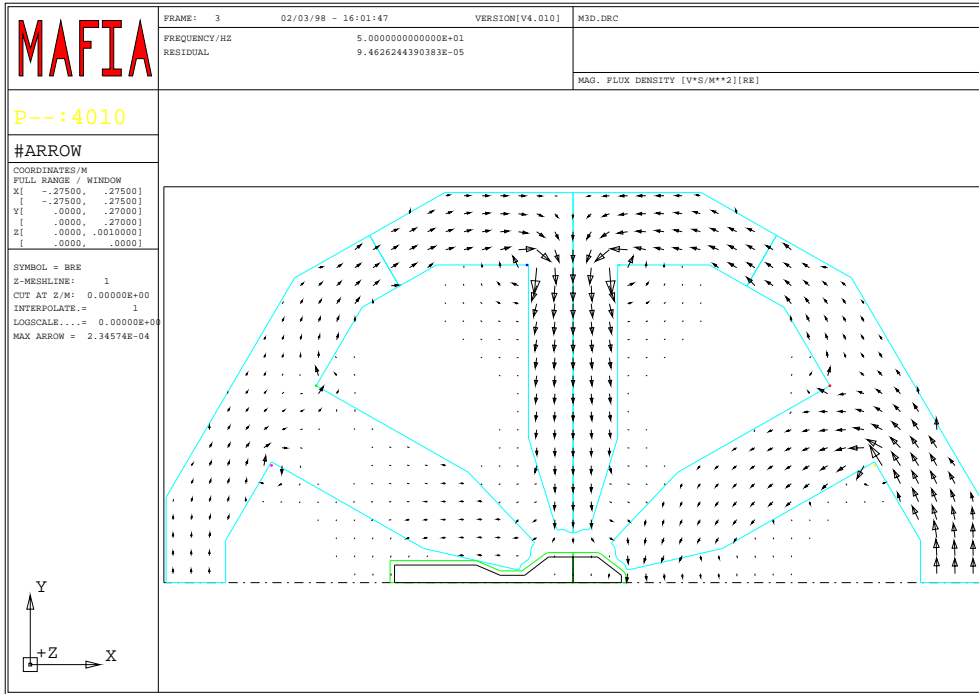


Figure 10: Vertical polarization: Distribution of the magnetic flux at 50 Hz

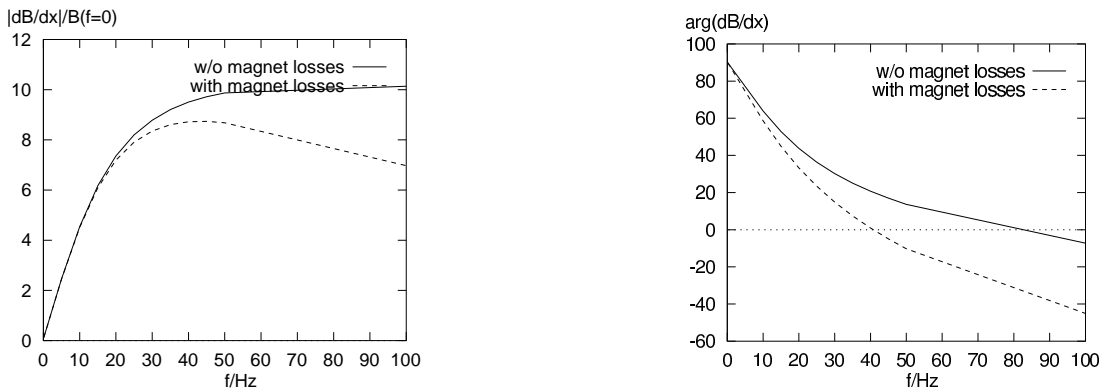


Figure 11: Vertical polarization: Quadrupole momentum in the field normalized to the static dipole field versus frequency in the vacuum chamber. Two cases are shown, one including only eddy current losses in the vacuum chamber, with and without magnet losses.

## Summary

For the SLS feed back system, it is planned to integrate the corrector magnets into sextupole magnets. Here, calculations of the behaviour due to eddy current losses are presented. They assume, that the mutual coupling between corrector and sextupole coils are zero, that is, opposite sexupole coils are connected in series.

The relationship between between the thickness of the magnet lamination can be described analytically, for the steel type given, a thickness of 1 mm or less is to be preferred.

The influence of eddy currents on the vacuum chamber wall has been computed via a MAFIA eddy current simulation. Due to the shape of the vacuum chamber, the vertical and horizontal magnetic polarization exhibit different behaviour. In the horizontal case, the attenuation and phase shifts are relatively feeble, whereas for vertical polarization, eddy current losses and, caused by them, field attenuation and phase slips are stronger.

Additionally the unsymmetric distribution of the wall current lead to transient quadrupole moments during the build up of the corrector field, which are not present for horizontal case. Beam dynamics simulations have shown, that these spurious effects have only a negligible influence on quality of the beam.

## References

- [1] FAX from Tesla Engineering Limited dated 27 January 1998
- [2] M. Werner, personal communication

# Appendix

## Electron beam distortions from induced quadrupole moments

Andreas Streun, 09. March 1998

The MAFIA calculations had shown that the asymmetry of the SLS storage ring vacuum chamber leads to induction of a quadrupole moment from variation of the horizontal correctors (i.e. vertical dipole field). There is no corresponding induced quadrupole moment from the vertical correctors, since the vacuum chamber is symmetric to the  $y = 0$  plane.

The magnitude of the peak induced gradient (step response) relative to the corrector's steady state dipole field was found to be  $\text{dB}/\text{dx} (t=0) = 13\text{m}^{-1} B_o (t \rightarrow \infty)$  (see page 8).

For the integrated strength of the spurious quadrupole this gives

$$\mathbf{k} \cdot \mathbf{l} = 13\text{m}^{-1} \Delta\vartheta,$$

with  $\Delta\vartheta$  [in rad] the angle of horizontal correction. This relation is a worst case estimate, since it assumes operating the correctors at highest frequency and full amplitude. In reality however we may expect a major DC part of the correction and smaller AC parts.

Two simple tests were done to investigate the effect on the stored beam. Time dependency was not taken into account, since the maximum corrector frequency of approx. 100 Hz is much lower than the SLS storage ring revolution frequency of 1.04 MHz. Instead the induced quadrupole moment was assumed to be constant. The program TRACY-2 was used for the calculations since its flexibility allows to set easily all kinds of correlations. Lattice file was SLS in the so-called D0-mode with dispersion free straight sections and with the »new« corrector layout, i.e. 72 correctors in sextupoles RIMA-SD, SE, SLB, SMB, SSB.

### First test: Residual closed orbit

Large displacement errors were set: 300  $\mu\text{m}$  for the girder joints, 100  $\mu\text{m}$  for the internal joint play, 50  $\mu\text{m}$  for the magnets and BPMs relative to the girder (all rms with cut at  $2\sigma$ ) (for definition of errors see the SLS design handbook). The closed orbit was centered in the BPMs by powering the correctors. Then the quadrupole moments were applied to the horizontal correctors. Since the correctors and BPMs are not at identical locations (but close to each other) this causes to some extent a distortion of the orbit due to dipole downfeed from the induced quadrupoles. Results are shown in the figures A1 to A4:

Fig. A1: Uncorrected closed orbit, shown for every lattice location (not only at BPMs).

Fig. A2: Closed orbit after correction, residual amplitudes between BPMs are visible, of course at BPMs the orbit was centered to zero.

Fig. A3: Closed orbit with induced quadrupoles and no further correction. There is no visible difference to fig. A2, since the orbit excursions between BPMs are dominating anyway the additional orbit distortion due to dipole downfeed.

Fig. A4: Closed orbit with induced quadrupoles only shown at the BPMs: The orbit that had been zeroed shows rather small amplitudes of  $<50\mu\text{m}$  in the horizontal and  $<200\mu\text{m}$  in the vertical. These amplitudes are relevant only immediately after switching on the corrector and decay with the same time constant as the dipole field builds up.

## Second test: Tune shift

Moderate displacements were set:  $200\mu\text{m}$  for the girder joints,  $10\mu\text{m}$  for the internal joint play,  $30\mu\text{m}$  for the magnets and BPMs relative to the girder (settings as used in the design handbook).

Output values are the average rms closed orbit measured at BPMs and the lattice tune before correction, after correction, and after introducing the induced quadrupole components without any further correction. 100 seeds were averaged.

Results:

	horizontal	vertical
uncorrected		
$\langle\sigma_{\text{CO}}\rangle [\mu\text{m}]$	2032	3294
corrected		
$\langle\sigma_{\text{CO}}\rangle [\mu\text{m}]$	0.004	0.016
$\langle\Delta Q\rangle$	0.00163	0.00001
$\sigma_{\Delta Q}$	<b>0.0068</b>	<b>0.0054</b>
with induced quadrupoles:		
$\langle\sigma_{\text{CO}}\rangle [\mu\text{m}]$	10.4	8.3
$\langle\Delta Q\rangle$	0.00005	-0.00008
$\sigma_{\Delta Q}$	<b>0.0073</b>	<b>0.0060</b>

The additional average rms closed orbit distortion due to induced quadrupoles is about  $10\mu\text{m}$  in both planes. The *additional* rms tune shift due to induced quadrupoles is comparable to the rms tune shift after closed orbit correction alone. The square sum of rms tune shifts from closed orbit correction alone and from the induced quadrupoles is an upper limit for tune variations to be expected when one would wildly switch on and off the correctors at full amplitude. Even for this extreme and unrealistic situation the rms full tune shift of  $<0.01$  in both planes is small compared to the amplitude dependant ( $\approx 0.05$ ) and higher order chromatic ( $\approx 0.3$ ) tune shifts.

## Conclusion

Induced quadrupoles from variation of horizontal correctors were studied in two simplified worst-case scenarios. The effect on orbit and lattice tune turned out to be rather small. Thus redesign of the vacuum chambers in order to suppress the effect seems not necessary.

